iJRASET
International Journal For Research in Applied Science and Engineering Technology

INTERNATIONAL JOURNAL FOR RESEARCH

IN APPLIED SCIENCE & ENGINEERING TECHNOLOGY

Volume: 7 **Issue:** IX **Month of publication:** September 2019

DOI: http://doi.org/10.22214/ijraset.2019.9026

www.ijraset.com

Call: 08813907089 | E-mail ID: ijraset@gmail.com

International Journal for Research in Applied Science & Engineering Technology (IJRASET)
ISSN: 2321-9653; IC Value: 45.98; SJ Impact Factor: 7.177
Volume 7 Issue IX, Sep 2019- Available at www.ijraset.com

Numerical Analysis of Thermal Friction Stir Welding (FSW) Application in Aerospace Industry

N Chakroun[1], A Noureddine[2], F Saidi[3], O Mimouni[4]
[1, 2]*National Polytechnic School of Oran Maurice Audin, Mechanical Engineering Department.*
[3]*Department of Maritime Engineering, University of Sciences and technology of Oran, Mohamed Boudiaf. Naval Aero-Hydrodynamics Laboratory.*
[4]*Lecturer at the Department of Aeronautics University of Blida*

***Abstract:** In this work, Friction Stir Welding (FSW) of 2017A-T451 aluminum alloy for a constant tool rotational speed 1250 rpm is investigated and analyzed. 3D numerical simulation has been carried out with the aid of ANSY code. In this context, two steps are performed; a mesh system is adapted to the geometry (plaque and tool) in order to use the finite elements. Secondly; the predicted result of plate temperature has been compared to experimental result. The surface temperature of the plate increases with the passage of the rotating tool; this is due to the increasing of friction between the tool and plate. This increase is slow until 300 s then it decreases rapidly. A good agreement is noted between the experimental and predicted results. According to this result, ANSYS provides a satisfactory prediction for the FSW.*
***Keywords:** Friction Stir Welding (F.S.W.), modeling, finite element (F.E), ANSYS, Aerospace Industry, Alloy 2017A- T451 Friction Stir Welding (F.S.W.), modeling, finite element (F.E), ANSYS*

I. INTRODUCTION

The use of the FSW for the assembly of aluminum alloy structures has many attractions for the industry especially the aeronautics constructions [1]. This assembly is released by friction and kneading of the material of the sheets to be welded without the additional material and without employ an external heat source in contrast to traditional welding techniques such as arc welding and Laser welding [2]. The FSW process is especially suited to aluminum alloys and other metal alloys known to be difficult to weld with conventional methods.

The welding with FSW is carried out without reaching the melting temperature of the base metal which is not achievable with the usual welding processes [3]. Indeed, during FSW welding, the surface temperature in the materials is much lower than the melting temperature [4].

This makes it possible to obtain a quality of welding which is clearly superior to other techniques [5]. Zadpoor et al. [6] and Ericsson et al. [7] found that the FSW joint remains higher than that of the conventional fusion weld joints. This was affirmed by the study of Yong et al. [8] who establish a conclusion that a higher exhaustion in the FSW joints compared to that of Metal Inert Gas weld joint.

In this respect, the FSW remains a complex phenomenon, for that we need to study the thermal behavior of the combined system tool-plate, because the welding temperature affects the quality and efficiency of welding [9]. Moreover, it is very difficult to perceive of the joint during the forming process [10].

However, the numerical simulation overcome this problem by providing an effective way to analyze closely the FSW procedure [11-12]. In this context, Prasanna et al. [13] has analyzed the thermo-mechanical of the aluminum Alloys with zinc as the primary alloying element (7075-T651) this process is carried out using the finite element code by.

On the other hand, Cavaliere et al [14] and Colegrove et al. [15] studied the effect of the Tool Geometries on Thermal Analysis of the Friction Stir Welding

This article aims to investigate and analyze numerically the FSW, including welding processes, temperature distribution and residual stresses.

The predicted surface temperature is compared with the experimental work of Mimouni et al [16]. The mesh procedure and the boundary conditions are discussed. FSW's numerical simulation simulates the FSW welding process to predict the various parameters of the system. The contours of temperature and constraints of Von Mises are discussed and illustrated by a case study.

ISSN: 2321-9653; IC Value: 45.98; SJ Impact Factor: 7.177
Volume 7 Issue IX, Sep 2019- Available at www.ijraset.com

II. MATERIAL AND GEOMETRY

In this section, the approach used for the numerical simulation of the FSW process is presented. Two steps are elaborate to release this study; firstly, a mesh system is adapted to the geometry (plaque and tool). Two rectangular shaped plates are used as parts to be welded is illustrated in the figure 1. The dimensions have been reduced to reduce the simulation time. The size of the plates is identical 250 x 100 x 4 (mm3).

The diameter of the shoulder of the tool is 22mm. The size of the tool is equal to the diameter of the shoulder.

The thermal and mechanical properties of plate 2017A- T451 are summarized in the Table 1 and Table 2 [16].

Table 1. Mechanical properties of 2017A plate

Properties	Values
E (MPa)	70e9
μ	0.3
A (mi-crons/m°C)	24.5e-6

Table 2. Thermal properties of 2017A

T (°C)	20	100	200	300	400	510
λ (W/m°C)	135	165	185	207	222	220
Cp(J/kg°C)	866	915	949	1041	1178	1276
ρ (kg/m3)	2805	2795	2770	2750	2700	2700

While, the mechanical characteristics of the tool used in this process is presented in Table 3 [16].

Table 3. The properties of steel (Tool)

Properties	Values
E (MPa)	193e9
μ	0.3
λ (W/m°C)	16
Cp (J/kg°C)	500
ρ (kg/m3)	7480

A. Computational Grid

In order to release the numerical simulation of the FSW, a mesh is adapted to resolve the finite element method. The element used for the simulation of the plates and the tool is the element SOLID226 used for the simulation of coupled phenomena (structural-thermal) (Figure 2).

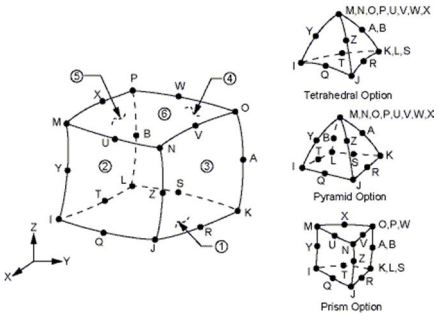

Fig.2. Finite element SOLID226.

ISSN: 2321-9653; IC Value: 45.98; SJ Impact Factor: 7.177
Volume 7 Issue IX, Sep 2019- Available at www.ijraset.com

A hexahedron mesh is carried out instead of a tetrahedral mesh to avoid dependence on the direction of the mesh12. For more accurate results, a finer mesh is used in the area of the weld line as shown in the Figure 3.

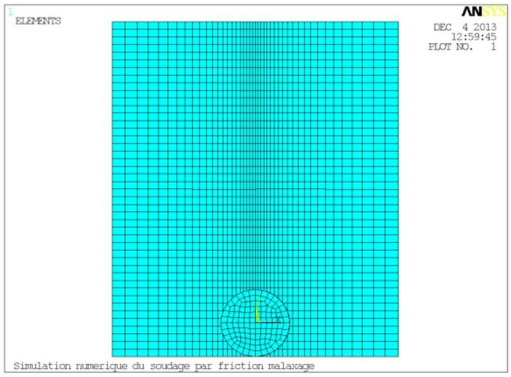

Fig 3. Meshing of the two plates and FSW tool

Secondly, a direct coupled ANSY solver is executed to analysis the phenomena the in the second step.

III. BOUNDARY CONDITIONS

To perform this simulation, it needs a boundary conditions such as thermal boundary conditions and mechanical boundary Conditions.

A. Thermal Boundary Conditions

The thermal condition is illustrated in the figure 4. Convection describes the heat loss to the environment. Conduction losses also occur on the underside of the plates.

Equation (1) describes the steady-state heat transfer in the plate where a convective term (right-hand side) is included to account for the effect of material movement

$$\nabla.(k\nabla T) + q = \rho C p V T.\nabla T \qquad (1)$$

q represents the rate of heat source per volume; VT is the welding (transverse) speed.

The model simulates the heat dissipation due to the interaction among the tool's pin and shoulder with the workpiece (surface heat of friction and volumetric heat of deformation) as a surface heat flux (space mapping) in the tool pin and shoulde[15]:

$$Q_{pin}(T) = \begin{cases} \frac{\mu}{\sqrt{3(1+\mu^2)}}\, r_p\, \omega \bar{Y}(T) & : T < T_{melt} \\ 0 : T > T_{melt} \end{cases} \qquad (2)$$

Q (W/m2) is the pin heat flux and μ is the friction coefficient between the pin and the workpiece, rp denotes the pin radius, ω refers to the pin's angular velocity (rad/ s), and $\bar{Y}(T)$ is the average shear yield stress of the material as a function of temperature.

B. Mechanical Boundary Conditions

The object is now fixed in each plate. The retained parts (plates) are blocked in all directions. To simulate pressing the lower surfaces of the plates, all lower nodes of the object are stuck in the perpendicular direction (z direction) is presented in Figure 5.

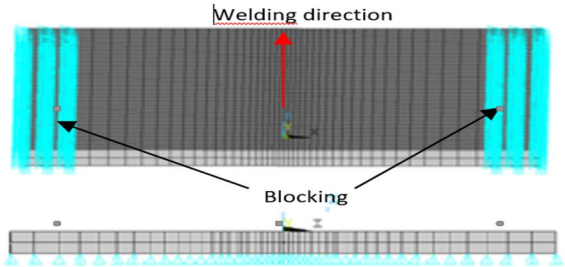

Fig 5. Mechanical boundary conditions

ISSN: 2321-9653; IC Value: 45.98; SJ Impact Factor: 7.177
Volume 7 Issue IX, Sep 2019- Available at www.ijraset.com

C. *Welding Conditions*

The FSW process consists of three primary phases as Follow [17].

1) *Plunge Phase:* the rotating tool slowly into the material until the shoulder of the tool touches the material.
2) *Moving Phase:* turning tool moves along the weld line. During this phase, there's a rise in temperature after the welding line, but the maximum temperature values do not exceed the melting temperature of the metal
3) *Shrinkage Phase:* This phase is characterized by the end of the welding operation and the shrinkage of the tool from the material.

These phases described above are summarized in the Table 4.

Table 4. Welding conditions

Step	Time (s)	Conditions	Speed
1	2	Plunge	ω= 1250 rpm
2	15	Moving	V= 5 mm/s
3	25	Shrinkage	/

IV. RESULTS AND DISCUSSION

A. *Model Evaluation*

Figure 6 show the temperature evolution of depending on the welding time. A good agreement is noted between the experimental and predicted results. The temperature of the plate increases with the passage of the welding tool. i.e. increasing of friction between the tool and plate. This increase is slow until 300 s then it decreases rapidly.

According to this result ANSYSprovides a satisfactory prediction for the temperature.

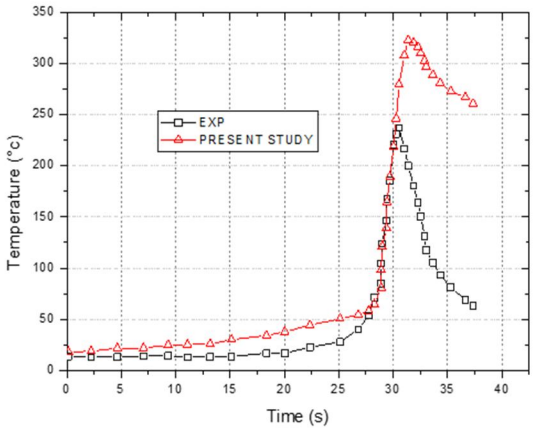

Fig 6. Comparaison of predicted and experimenntal temperature evolution according to welting time

B. *Temperature Distribution*

The results of the numerical simulation for the second and third phases of the process are respectively shown in Figures 7 a-b. The distribution of the temperature field under the FSW tool increases then decreases to reach low values away from the tool.

The maximum temperature on the welding line is of the order of 416 ° C. at the end of the third phase (Figure. 7.b), whereas this temperature is lower than the melting temperature of the indicated aluminum at 620 ° C. In addition, the heat generated on the plate is due to mechanical loads (friction). This condition clearly shows the pasty state reached by aluminum at this temperature. We note that no external heat source is used.

Indeed, a control of the load exerted (coefficient of friction) on the plate by the tool was carried so that the temperature of the plate does not exceed the melting temperature of the aluminum. Indeed, the temperature increases, the material softens, and the coefficient of friction decreases.

ISSN: 2321-9653; IC Value: 45.98; SJ Impact Factor: 7.177
Volume 7 Issue IX, Sep 2019- Available at www.ijraset.com

After the analyses, the heating observed in this model asserts that the generation of heat during the welding operation is due to the friction between the tool shoulder and the part to be welded.

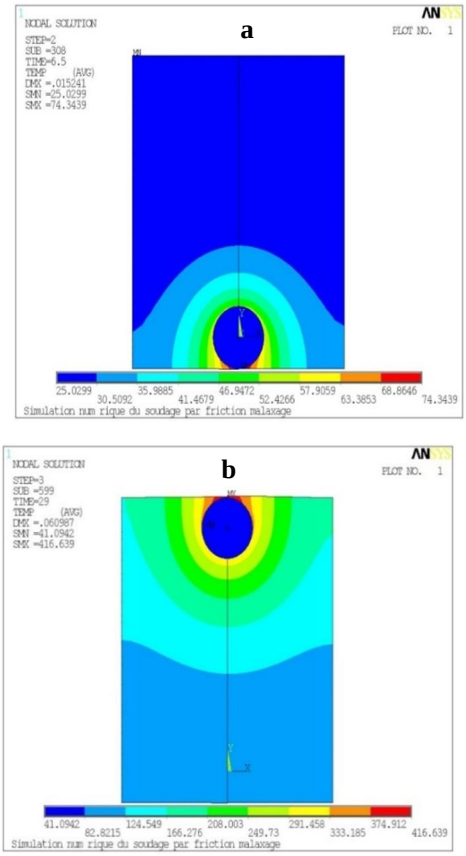

Figure 7. Distribution of temperatures at the second phase (a) and third phase (b)

C. Von Mises Constraints

The figure 8 a-b show the distribution of the equivalent Von Mises stresses. The stresses are mainly located in the weld bead (core) and its vicinity (ZATM, ZAT). It is noted that the maximum value of the Von Mises stresses has reached 317 Mpa, which is far away of the breakdown value of aluminum 2017-T451 (475 Mpa). This concentration is essentially over the zone of the nucleus where it has a maximum mixing of the material and this value diminishes as one moves away from the mixing zone until reaching a value of 141Mpa.

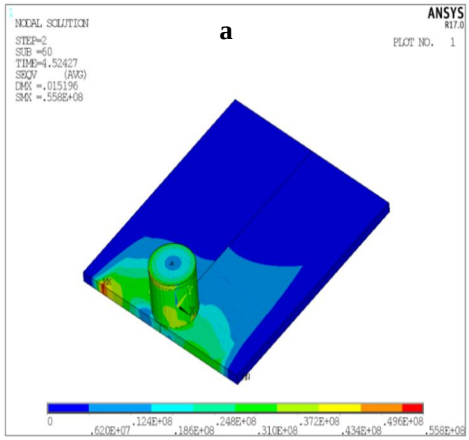

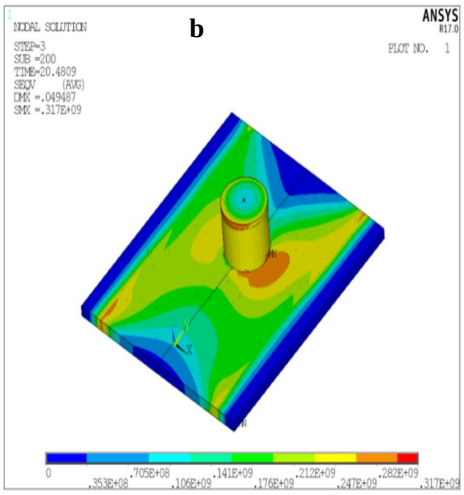

Figure 8. Von Mises Constraints distribution at the second phase (a) and third phase (b)

V. CONCLUSION

The implementation in the finite element code ANSYS thermo-mechanical model taking into account the welding parameters (tool geometry, plate thickness, speed, feed rate, plunge effort and type of material to be welded) was performed. The study on contact management has helped to highlight the difficulties in choosing the type of contact. However, it seems that for the warming, the nodal contact would be more appropriate than the surface contact.

The tool rotational speed during friction stirs welding of the investigated alloy affect significantly the weld joint temperature.

Furthermore, computer simulations can predict the temperature fields for acceptable computation times from a material point of view. These results are comparable to those obtained experimentally. The set of results obtained seem to agree well with the numerical and experimental data already published, in particular the temperature distribution.

However, other studies, carried out using an E.F. code based on fluid mechanics are required to predict the quality of the weld through the study of the flow of material around the tool. The use of different programs according to the nature of the desired results is now essential to treat different physical phenomena caused by the F.S.W. welding operation (Temperature field, de-formation).

VI. ACKNOWLEDGEMENT

We would like to express our special thanks of gratitude to the prof Benamar Ali of the National Polytechnic School of Oran Maurice Audin, Mechanical Engineering Department.

REFERENCES

[1] W. Cassada, J. Liu, J. Staley. Aluminum alloys for aircraft structures. December 2002 Advanced Materials and Processes 160(12):27-29
[2] Precipitation and plasticity couplings in a 7xxx aluminium alloy: application to thermomechanical treatments for distortion correction of aerospace component. https://tel.archives-ouvertes.fr/tel-00502536/document. Date accessed: 2009.
[3] Watanabe T, Takayama H, Yanagisawa A. Joining of aluminum alloy to steel by friction stir welding. Journal of Materials Processing Technology. 2006, 178, pp. 342-349.
[4] Santiago D, Urquiza S, Lombera G, de Vedia L. 3D Modeling of material flow and temperature in Friction stir welding. Soldagem & Inspeção. 2009, 14, pp. 248–256.
[5] Suri A. An Improved FSW Tool for Joining Commercial Aluminium Plates. Procedia Materials Science. 2014, 6, pp. 1857–1864
[6] Zadpoor A, Sinke J, Benedictus R. The effects of friction stir welding on the mechanical properties and microstructure of 7000 series aluminium tailor-welded blanks. International Journal of Material Forming. 2012, 1, pp. 1311–1314.
[7] Ericsson M, and Sandstro ¨m R,Int J Fat 25 (2003) 1379.
[8] Yong Z, Zhengping L, Keng Y, and Linzhao H, Mater Des 65 (2015) 675.
[9] Mishra RS. Friction Stir Welding and Processing. Materials Science and Engineering: R: Reports. 2005, 50 (1-2), pp. 1-78.
[10] D. Jacquin, B. de Meesterb, A. Simar, D. Deloison, F. Montheillet, C. Desrayaud. A simple Eulerian thermomechanical modeling of friction stir welding. Journal of Materials ProcessingTechnology. 211. 2011. 57-65
[11] Song M, Kovacevic R. Thermal modeling of friction stirs welding in a moving coordinate system and its validation. International Journal of Machine Tools and Manufacture. 2003, 43, pp. 605- 615.

[12] Atharifar H, Lin DC, Kovacevic R. Numerical and Experimental Investigations on the Loads Carried by the Tool During Friction Stir Welding. Journal of Materials Engineering and Performance. 2009, 18 (4), pp. 339-350.
[13] Prasanna P, Rao BS, Rao GK. Finite Element Modeling for Maximum Temperature in Friction Stir Welding and its Validation. Journal of Advanced Manufacturing Technology. 2010, 51, pp. 925-933.
[14] Cavaliere P, Nobile R, Panella F, Squillace A. Mechanical and microstructural behavior of 2024-7075 aluminium alloy sheets joined by friction stir welding. International Journal of Machine Tools and Manufacture. 2006, 46, pp. 588 – 594.
[15] Colegrove PA, Shercliff HR. Development of Trivex friction stir welding tool part 1: two-dimensional flow modelling and experimental validation. Science and Technology of Weldingand Joining. 2004, 9, pp. 345-351.
[16] Mimouni O, Badji R, Kouadri-David A, Gassaa R, Chekroun N, Hadji M. Microstructure and Mechanical Behavior of Friction-Stir-Welded 2017A-T451 Aluminum Alloy. Transactions of the Indian Institute of Metals. 2019, pp. 1-16.
[17] Cerri E, Leo P, Wang X, Embury J. Mechanical properties and microstructural Evolution of friction-stir-welded thin sheet aluminum alloys. Metallurgical and Materials Transactions. 2011, 42, pp. 1283–1295.

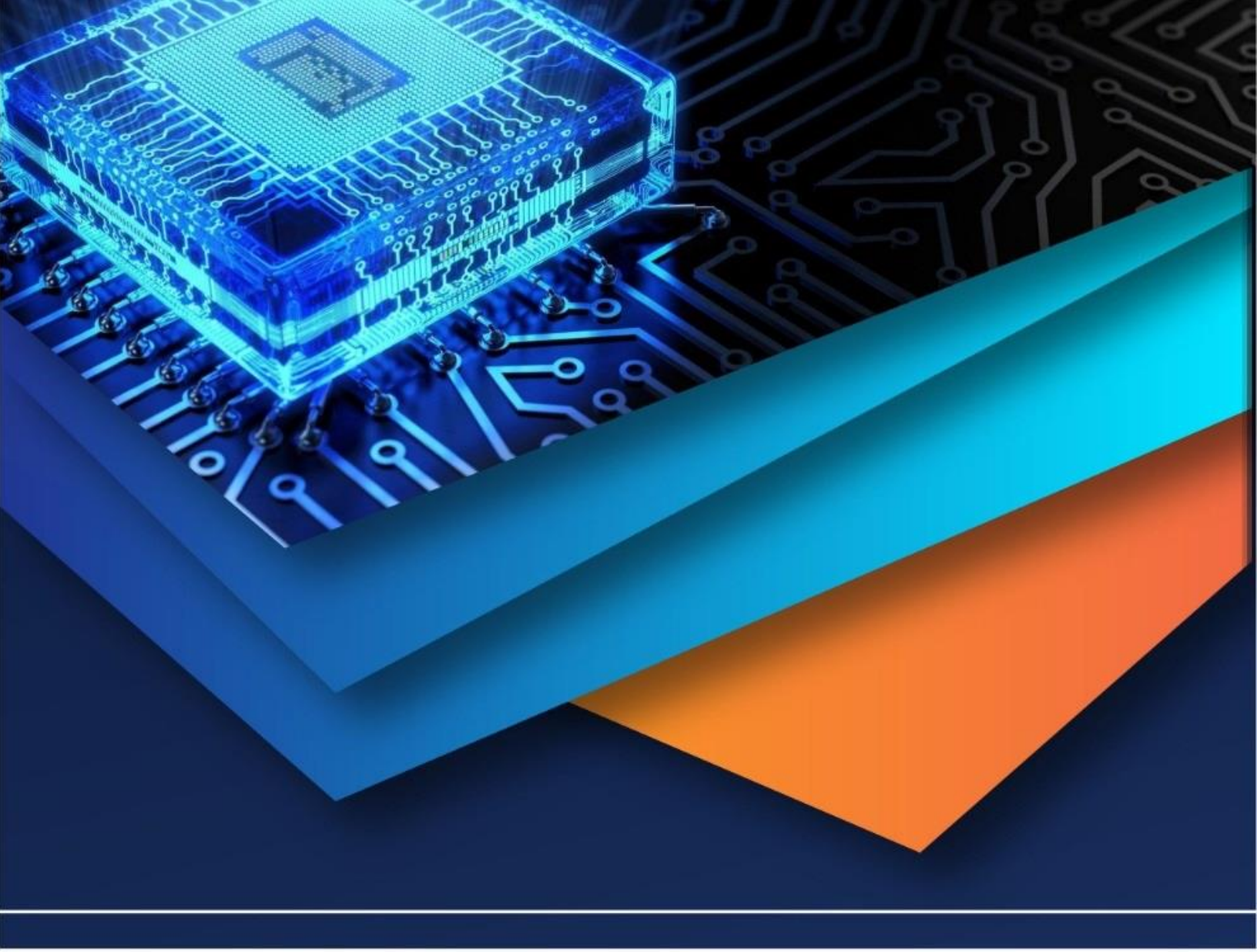

10.22214/IJRASET

45.98

IMPACT FACTOR: 7.129

IMPACT FACTOR: 7.429

INTERNATIONAL JOURNAL FOR RESEARCH

IN APPLIED SCIENCE & ENGINEERING TECHNOLOGY